Available online at www.sciencedirect.com
ScienceDirect
Journal of Sound and Vibration 298 (2006) 651–671
JOURNAL OF SOUND AND VIBRATION
www.elsevier.com/locate/jsvi

Seated occupant interactions with seat backrest and pan, and biodynamic responses under vertical vibration

S. Rakheja[a,*], I. Stiharu[a], H. Zhang[a], P.-É. Boileau[b]

[a]*CONCAVE Research Centre, Concordia University, 1455 de Maisonneuve West, Montréal, Que., Canada H3G 1M8*
[b]*Institut de recherche Robert-Sauvé en santé et en sécurité du travail, 505 de Maisonneuve West, Montréal, Que., Canada H3A 3C2*

Received 8 May 2006; received in revised form 10 May 2006; accepted 8 June 2006
Available online 4 August 2006

Abstract

The relative interactions of the seated occupants with an inclined backrest were investigated in terms of apparent mass (APMS) responses at the two driving-points formed by the buttock–seat pan and the upper body-backrest under exposure to broad-band and road-measured vertical vibration. The measurements were performed using 24 adult subjects seated with full contact with the back support and two different positions of the hands (in lap and on steering wheel), while exposed to three different levels of broad band (0.25, 0.5 and 1.0 m/s^2 rms acceleration) vibration in the 0.5–40 Hz frequency range, and a track-measured vibration spectrum (1.07 m/s^2 rms acceleration). The forces developed on the seat pan and the backrest in directions normal to the supporting surfaces were measured to derive the APMS responses at both the driving-points. The results showed significant interactions of the upper body with the back support in a direction normal to the backrest, even though the vibration is applied along the vertical axis. At low frequencies, the backrest APMS magnitude was smaller than that measured at the seat pan, but it either exceeded or approached that of the seat pan APMS in the vicinity of the primary resonant frequencies. The results also suggested considerable effect of the hands position on the APMS magnitudes measured at both the driving-points. The effects of variations in the excitation type and magnitude, considered in this study, were observed to be small compared to those caused by the hands position and individual body masses. Owing to the strong effects of the body mass on the measured APMS responses at both driving-points, a total of 8 target data sets were identified corresponding to four mass groups (<60, 60.6–70, 70.5–80 and >80 kg) and two hands positions for formulating mechanical equivalent models. The model parameters identified for the target functions suggested that the models mass, stiffness and damping parameters increase with increasing body mass. The observed variations in the identified parameters could be applied for predicting the APMS responses reflected on the pan as well as backrest of the human occupants with specific body mass.

1. Introduction

Seated occupants interactions with the seat, while exposed to vertical vibration, have been mostly characterized on the basis of the force–motion relationship at a single driving-point formed by the seat-pan and the body interface. The occupant's responses to vertical vibration have been conveniently expressed in

*Corresponding author.
E-mail address: rakheja@vax2.concordia.ca (S. Rakheja).

0022-460X/$ - see front matter © 2006 Elsevier Ltd. All rights reserved.
doi:10.1016/j.jsv.2006.06.025

terms of apparent mass (APMS) or driving-point mechanical impedance (DPMI), derived from the dynamic force and motion measured at the seat pan under a variety of test conditions, involving differences in subjects' mass, sitting posture, and frequency, magnitude and type of vibration [1–3]. A great number of studies have characterized the biodynamic responses of subjects seated without a back support, thereby justifying the consideration of a single driving-point at the buttock–seat interface [4–6]. A coupled occupant-seat system in a whole-body vibration environment constitutes multiple driving-points, where the vibration enters the body at the buttocks, hands, feet and the back. While the biodynamic responses are mostly derived on the basis of the buttock–seat pan interactions alone, a few studies have shown strong influences of back support conditions suggesting considerable dynamic interactions of the upper body with the backrest.

Some studies have reported considerable effects of the sitting posture, as determined from muscle tension, back support condition and the seat geometry, on the biodynamic responses [4,5,7–9]. Variations in the postural conditions and supports alter the curvature of the spine and thereby the stiffness and energy dissipation properties. An erect sitting posture yields higher magnitudes of DPMI in the vicinity of the observed resonant frequencies than those attained with a relaxed sitting posture [7]. Higher resonant frequency of the occupant sitting with a more erect or tense posture has also been reported in other studies [8,9]. The biodynamic responses of individuals seated on a flat pan against a vertical backrest have also been quantified in a few studies [10–15]. It has been shown that sitting with a back support results in increase in rotational motion of the upper body, and magnitudes of APMS and vibration transmitted to the head at frequencies above 5 Hz. These studies have also shown that sitting against an inclined backrest, such as that provided by the automotive seats, yields higher APMS magnitude and the corresponding primary resonant frequency, when compared to those observed from data obtained for no back and vertical back support conditions [15]. These differences can be attributed to the additional dynamic interactions of the upper body with the backrest. Moreover, a posture with hands positioned on a steering wheel coupled with an inclined back support causes considerably lower peak magnitude of APMS and the corresponding frequency [15], which may be attributed to additional restraint provided by the hands for the upper body.

The analyses in the above studies, however, have been limited to single driving-point at the seat pan, while the interactions with the back support are ignored. Exposure to vertical vibration is known to yield considerable fore-aft and pitch motions of the upper body of the seated occupant [16], which tend to instigate increased level of dynamic interactions with the back support. The dynamic interactions of the human body seated with a vertical back support and exposed to vertical vibration have been measured in a recent study [17]. The study related the forces developed along the fore-aft and lateral axes at the backrest and the pan to the acceleration due to vertical vibration to drive cross-axis APMS due to horizontal forces. The study established the presence of high magnitude forces at the vertical backrest and the seat pan in the fore-aft direction.

An inclined backrest would be expected to yield higher degree of interaction between the upper body and the backrest, as it tends to support relatively larger portion of the body mass and provide greater contact with the body. Moreover, the backrest serves as the secondary source of vibration along the direction normal to the backrest, particularly when the backrest inclination is relatively large as in the case of automotive seats, even under pure vertical vibration. The characterization of the biodynamic response of seated occupants exposed to vertical vibration thus requires the analyses of dynamic interactions of the seated body with the backrest and the pan in terms of force–motion relationships at the two driving-points. This would be desirable to formulate effective mechanical-equivalent biodynamic models in support of on-going efforts for developing anthropodynamic manikins for assessment of seats [18].

In this study, dynamic interactions of the seated body with the seat are measured under vertical vibration in terms of forces developed at the pan and the backrest along the vertical and fore-aft axis, respectively. The measurements are performed using a total of 24 adult individuals under postural and vibration conditions considered representative of those applicable to automobile drivers and passengers. The measured data are analyzed to derive APMS characteristics reflected at the two important driving-points formed by the seat pan and the backrest, as functions of the body mass, hands position, and magnitude of broad-band random vertical vibration in the 0.5–40 Hz frequency range. A non-dimensional mechanical-equivalent model is proposed to characterize both the APMSs, and its validity is demonstrated through comparisons of the seat pan and backrest APMS responses with the mean measured data for occupants within different body mass ranges.

2. Experimental methods

2.1. Apparatus

A rigid seat structure was designed to mimic a typical automotive seat geometry and thus the sitting posture. The seat structure comprised of square tubes to reduce its weight and to achieve its fundamental natural frequency well above 40 Hz. The seat provided a 450 mm × 450 mm pan with inclination β of 13° with respect to a horizontal axis. A 450 × 500 mm aluminum plate served as the backrest. The angle between the seat pan and the backrest was 101°, as shown in Fig. 1, which yields the backrest inclination α of 24° with respect to the vertical axis. Two identical 222 N force transducers (Sensotec, model 41) together with a summing junction were installed between the backrest and the tubular support structure of the seat to measure the forces along an axis normal to the back support surface. The cross-axis sensitivity of the sensors was specified as very low, in the order of 3%. The seat assembly was installed on a vertical vibration simulator through a force platform consisting of four identical force sensors (Sensotec, model 41), each rated at 444 N, and a summing junction to measure the total vertical force developed at the seat base. The seat with the force platform provided a seat pan height of 220 mm, measured from the base of the backrest to the simulator platform. The seat and the force platform were positioned to achieve the overall center of gravity of the seat-occupant system near the geometric center of the force sensors. The mass of the assembly including base plate, seat structure, seat pan,

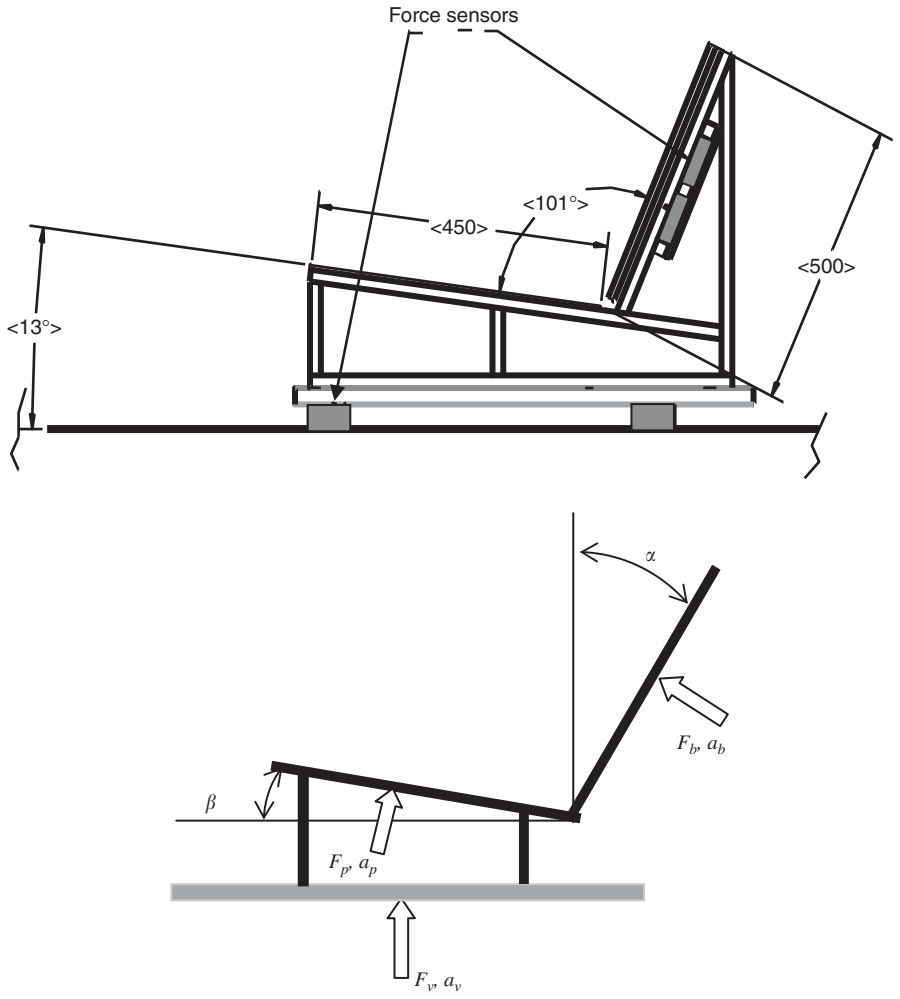

Fig. 1. A schematic of the test seat apparatus.

backrest and two backrest force sensors was measured as 36 kg. A steering column was also installed on the vibration simulator through a support structure to perform measurements with postures involving hands placed on the steering wheel. The steering column formed an angle of 23° with respect to the simulator surface, as illustrated in Fig. 2. The primary resonance frequency of the assembly comprising seat with its support structure, and the vibration platform with the steering column was measured as 45 Hz.

A single-axis accelerometer was installed on the seat base to measure acceleration due to vertical vibration excitation. The application of a pure vertical vibration at the seat base would yield components along axes normal to the seat pan and the backrest, which are related to the applied vertical acceleration, such that:

$$a_b = a_v \sin(\alpha),\ a_p = a_v \cos(\beta), \tag{1}$$

where a_v is magnitude of vertical acceleration measured at the seat base, a_b and a_p are magnitudes of acceleration components normal to the inclined backrest and pan, respectively, as shown in Fig. 1.

On the basis of the measurements of forces due to seated occupants developed at a vertical backrest along the three axes, it has been shown that the vertical and lateral force components are significantly smaller than the fore-aft component [17]. The body interactions with the backrest thus mostly occur along an axis normal to the backrest. The APMS responses at the seat pan and the backrest driving-points can be defined from the ratios of dynamic forces developed at the interfaces to the corresponding accelerations, both being measured along the axes normal to the pan and the backrest, such that:

$$M_p(\mathrm{j}\omega) = \frac{F_p(\mathrm{j}\omega)}{a_p(\mathrm{j}\omega)},\ M_b(\mathrm{j}\omega) = \frac{F_b(\mathrm{j}\omega)}{a_b(\mathrm{j}\omega)}, \tag{2}$$

where $M_p(\mathrm{j}\omega)$ is complex APMS measured at the seat pan along an axis normal to the seat pan corresponding to angular frequency of excitation ω. $F_p(\mathrm{j}\omega)$ is the normal component of force acting on the seat pan, which is related to vertical force F_v measured by the seat base force platform, $F_p = F_v \cos(\alpha)$. Considering the geometric relationships between vertical and normal forces and accelerations, $M_p(\mathrm{j}\omega)$ also defines the vertical APMS of the seated body at the seat pan driving-point. In the above equation, Eq. (2), $M_b(\mathrm{j}\omega)$ is the complex APMS measured at the backrest driving-point along an axis normal to the backrest, which relates to the normal force $F_b(\mathrm{j}\omega)$ developed at the backrest and acceleration a_b.

2.2. Test matrix

The experiments were performed with a total of 24 (12 male and 12 female) subjects. All subjects were considered to be healthy with no signs of musculo-skeletal system disorders. Table 1 summarizes the mean, standard deviation, minimum and maximum values of participants' age, body mass and height. The body

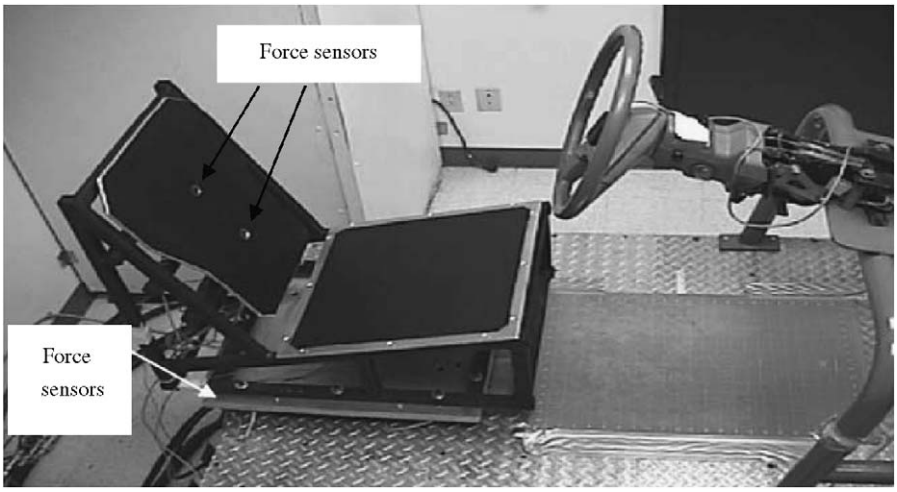

Fig. 2. A pictorial view of the test apparatus.

mass of the test subjects ranged from 48 to 111.4 kg, with mean body mass of 71.2 kg. The age of test subjects ranged from 21 to 53 years with mean age of 39.3 years.

Each subject was advised to sit on the test seat assuming a comfortable posture while making full use of the back support. The measurements were performed for the subject assuming two different sitting postures and exposed to two different types of vertical vibration excitations. The two postures were realized by placing the hands in lap (passenger-like posture, referred to as 'LAP') and on the steering wheel (driver-like posture, referred to as 'SW'), while maintaining the back in contact with the inclined backrest and feet resting flat on the vibration platform. The response characteristics were measured under different types and levels of excitations: white-noise random excitation in the 0.5–40 Hz range with overall rms accelerations of 0.25, 0.5 and 1.0 m/s^2, and random vibration measured at the seat base of an automobile on a relatively rough track at a speed around 70 km/h. Fig. 3 illustrates the acceleration power spectral density (PSD) of the vibration measured at the seat base of the automobile, derived using a bandwidth of 100 Hz. The spectrum reveals acceleration peaks near 1.3, 9 and 12 Hz, attributed to vertical mode resonance of the sprung mass, and the front and rear unsprung masses. The overall rms acceleration due to measured vibration was computed as 1.07 m/s^2. Each experiment was performed twice. The resulting test matrix thus included a total of 16 tests which were performed on each subject in order to characterize the influence of nature and magnitudes of vibration and hands position on the seat pan and backrest APMS responses.

2.3. Determinations of seat-pan and backrest APMS responses

The measurements were initially performed on the seat alone under selected excitations. The vertical APMS response of the seat and fore-aft APMS of the backrest obtained from measured forces and accelerations revealed nearly constant magnitude and negligible phase response in the 0.5–40 Hz frequency range. This data was used to perform inertial correction of the APMS responses of the human subjects. For each subject assuming a posture with specified hands position, the body weight supported by the seat pan and the backrest

Table 1
Age, body mass and height of the participants

Gender	Male	Female	All
Variable	Mean (standard deviation, min, max)	Mean (standard deviation, min, max)	Mean (standard deviation, min, max)
Number	12	12	24
Body mass (kg)	78.5 (13.45, 58, 100)	63.9 (17.14, 48, 111.4)	71.2 (16.81, 48, 111.4)
Height (cm)	176.3(3.92, 169, 181)	165.4 (5.9, 153, 175)	170.9 (7.42, 153, 181)
Age (yr)	38.2 (8.8, 21, 53)	40.4 (9.3, 26, 52)	39.3 (8.9, 21, 53)

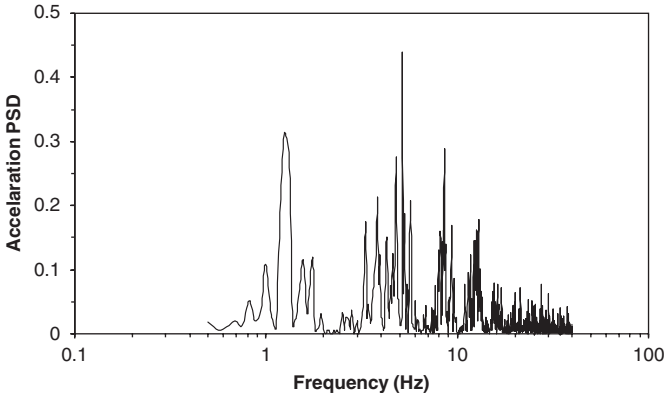

Fig. 3. PSD of acceleration in $(m/s^2)^2$/Hz due to vibration measured at the seat base of an automobile on a rough road.

were recorded from the static force signals displayed to the experimenter. These static force signals were also recorded after each test, and were compared with those recorded prior to the test to examine the consistency in the subject posture. The trial was repeated when difference in static forces acquired before and after a test exceeded 10%. The results revealed only slight variations in the static body forces measured for each subject before and after a trial, below 1%. The mean values of the two measurements were taken as the body masses supported by the two supporting surfaces.

The static force data revealed that the body mass supported by the seat pan ranges from 72.5% to 79.9% for male and from 74.9% to 80.8% for the female subjects, when the subjects are seated with their hands in the lap. The body mass supported by the backrest under same conditions varied from 25.2% to 38.4% for males, and from 24.9% to 40% for female subjects. Under the SW posture, the percent body mass supported by the pan and the backrest decreased slightly. The body mass supported by the seat pan ranged from 69.3% to 76.2% for males and from 71.5% to 78.1% for female subjects. The backrest under the same conditions supported 17.5% to 33.8% of the body mass for males, and from 19.7% to 37.6% for the female subjects. The mean values of the body mass supported by the seat pan and the backrest for male and female subjects were quite comparable under both postures, as evident in Table 2, while the backrest force data revealed larger variability, which could be attributed to variations in the use of back support and individual sitting habits.

The whole-body vehicular vibration simulator was operated to produce the motion signals corresponding to a selected excitation and the resulting force and acceleration signals were acquired using a multichannel signal analyzer. The validity of the vibration signal was examined by comparing its rms spectrum and overall rms acceleration with the target values [15]. These signals were subsequently used to compute the APMS response functions using Eq. (2). The vertical seat pan and backrest fore-aft APMS responses of the seated occupants were derived upon performing inertia corrections of the measured force data. The corrected real and imaginary components were analyzed to compute magnitude and phase responses corresponding to each test condition. A moving average, using 8 points, was then performed to smoothen the corrected APMS response data.

3. Mechanical-equivalent model

Considerable efforts are being made towards developments in anthropodynamic dummies that can characterize dynamic properties of vibration-exposed seated body, for routine evaluations of seats [18–21]. A number of lumped-parameter mechanical-equivalent models have been proposed on the basis of the measured biodynamic responses [1,22,23], which could serve as the essential basis for designing anthropodynamic dummies. The parameters of these models have been identified using the APMS data measured at the seat base, while the body interactions with the backrest are not considered. Moreover, the target biodynamic response data generally represents the mean response of the subject population with wide range of body masses. The strong dependency of the biodynamic response on the body mass has been widely reported in the literature [1,13,15,22,23]. Such models may thus yield close approximation of the biodynamic response for subject masses in the vicinity of the mean mass, while the applicability for automotive seating posture involving inclined back support may be questioned. International Standard, ISO-5982[6], has proposed a

Table 2
Mean and standard deviations of percent body mass supported by seat pan and backrest

Posture	Interface	% body mass supported: mean (standard deviation)		
		Male	Female	All
LAP	Pan	75.6 (2.3)	77.6 (1.9)	76.6 (2.3)
	Backrest	29.4 (3.0)	31.4 (5.5)	30.4 (4.7)
SW	Pan	72.4 (2.2)	74.5 (2.1)	73.5 (2.4)
	Backrest	27.9 (5.0)	28.2 (6.0)	28.1 (5.5)

baseline model considered applicable for mean mass near 75 kg. It further provides model parameters to define the APMS and impedance characteristics of body masses of 55 and 90 kg, by varying the mass parameters alone to satisfy the static body mass supported by the seat. Similar approach has also been applied to define model parameters of occupants in different body mass ranges, while seated assuming typical automotive seat postures [22].

The quality of a mechanical-equivalent model for automotive seating applications could be enhanced by considering the biodynamic responses measured at the two driving-points formed by the seat-buttock and upper body-backrest interfaces. Considering the strong effects of hands position on the measured biodynamic responses, it would also be desirable to identify two distinct models applicable for the LAP and SW postures. Owing to the most important dependence of the biodynamic responses on the body mass, a non-dimensional mechanical-equivalent occupant model is attempted to account for both the fore-aft backrest and vertical seat pan interactions in terms of measured APMS responses. Fig. 4 illustrates the structure of the baseline four-DOF model of the seated occupant with inclined pan and back support. The model structure also incorporates the geometric effects of a typical automotive seat, described in Section 2.2, and comprises three masses coupled by linear elastic and damping elements constrained to translate along the axes shown in the figure. The rotational stiffness and damping characteristics of the body are neglected, while linear spring and damping elements are introduced to represent the dynamic interactions of the upper body with the backrest. The friction between the upper body and the backrest surface is assumed to be negligible. Although the model is not intended to relate to anatomical structures of the human body, masses m_1 and m_2 may be considered to represent the upper body for the purpose of characterizing the back biodynamic response and computing the static weight on the seat back. The dynamic forces developed at the seat pan and the backrest under a vertical excitation x_i at the seat pan, can be derived as

$$F_p = m_0\ddot{x}_0 + (m_1\ddot{x}_1 + m_2\ddot{x}_2)\cos(\alpha - \beta), \tag{3}$$

$$F_b = m_1\ddot{y}_1 + m_2\ddot{y}_2. \tag{4}$$

The coordinates x_1 and x_2 define the motion of masses m_1 and m_2, respectively, along the x-axis (normal to the seat pan), and $x_0 = x_i \cos\beta$ is the displacement coordinate of the base mass m_0, as shown. y_1 and y_2 define the motions of masses m_1 and m_2, respectively, along an axis normal to the backrest.

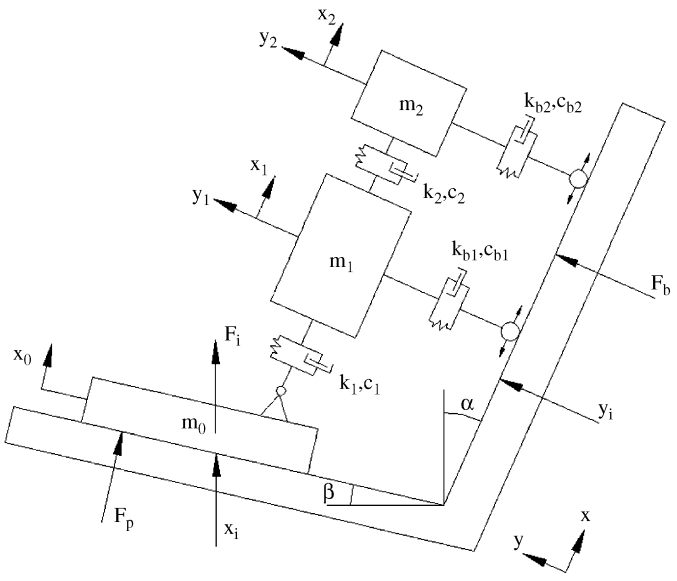

Fig. 4. Mechanical-equivalent biodynamic model of the seated occupant with back support.

The APMSs of the model at the seat-pan and the backrest are derived as

$$M_p^*(s) = m_0 + \left[m_1 \frac{X_1}{X_0}(s) + m_2 \frac{X_2}{X_0}(s)\right] \cos(\alpha - \beta), \tag{5}$$

$$M_b^*(s) = m_1 \frac{Y_1(s)}{X_i(s) \sin\,\alpha} + m_2 \frac{Y_2(s)}{X_i(s) \sin\,\alpha}, \tag{6}$$

where M_p^* and M_b^* are APMSs of the model computed at the two driving-points along the x- and y-axis, respectively, and $s = j\omega$.

A non-dimensional model may also be derived upon normalizing the model paramters with respect to the total body mass, M_T. The normalized seat-pan and backrest APMS responses of the model $\bar{M}_p^*$ and $\bar{M}_b^*$, may thus be expressed as

$$\bar{M}_p^*(s) = \mu_0 + \left[\mu_1 \frac{X_1}{X_0}(s) + \mu_2 \frac{X_2}{X_0}(s)\right] \cos(\alpha - \beta), \tag{7}$$

$$\bar{M}_b^*(s) = \mu_1 \frac{Y_1(s)}{X_i(s) \sin\,\alpha} + \mu_2 \frac{Y_2(s)}{X_i(s) \sin\,\alpha}, \tag{8}$$

where $\mu_i = m_i/M_T$ $(i = 0, 1, 2)$ are the non-dimensional model masses, which represent proportions of the total body mass.

The transfer functions in the above equations are derived as

$$\frac{X_1}{X_0}(s) = \frac{\mu_1\left(2\xi_1\omega_1 s + \omega_1^2\right)\left(s^2 + 2\xi_2\omega_2 s + \omega_2^2\right)\cos(\alpha - \beta)}{\left[\mu_1 s^2 + \left(2\xi_1\omega_1\mu_1 + 2\xi_2\omega_2\mu\right)s + \left(\omega_1^2\mu_1 + \omega_2^2\mu_2\right)\left(s^2 + 2\xi_2\omega_2 s + \omega_2^2\right)\right] - \left(2\xi_2\omega_2\mu_2 s + \omega_2^2\mu_2\right)\left(2\xi_2\omega_2 s + \omega_2^2\right)}, \tag{9}$$

$$\frac{X_2}{X_0}(s) = \frac{2\xi_2\omega_2 s + \omega_2^2}{s^2 + 2\xi_2\omega_2 s + \omega_2^2}\frac{X_1}{X_0}(s), \tag{10}$$

$$\frac{Y_1(s)}{X_i(s) \sin\,\alpha} = \frac{2\xi_{b1}\omega_{b1} s + \omega_{b1}^2}{s^2 + 2\xi_{b1}\omega_{b1} s + \omega_{b1}^2}; \quad \frac{Y_2(s)}{X_i(s) \sin\,\alpha} = \frac{2\xi_{b2}\omega_{b2} s + \omega_{b2}^2}{s^2 + 2\xi_{b2}\omega_{b2} s + \omega_{b2}^2}, \tag{11}$$

where ω_1 and ω_2, and ξ_1 and ξ_2 are the uncoupled natural frequencies and damping ratios, respectively, of model masses m_1 and m_2, along the x-axis, such that

$$\omega_i^2 = \frac{k_i}{\mu_i M_T}, \quad \xi_i = \frac{c_i}{2\mu_i\xi_i\omega_i M_T}, \quad i = 1, 2,$$

where k_1 and k_2 are the stiffness constants of springs constrained to translate along x-axis, and c_1 and c_2 are the viscous damping coefficients.

ω_{bi} and ξ_{bi} $(i = 1,2)$, in a similar manner, define the natural frequencies and the damping ratios, respectively, of the uncoupled masses m_1 and m_2, corresponding to motion along the y-axis, such that

$$\omega_{bi}^2 = \frac{k_{bi}}{\mu_i M_T} \quad \text{and} \quad \xi_{bi} = \frac{c_{bi}}{2\mu_i\omega_{bi} M_T}, \quad i = 1, 2,$$

where k_{b1} and k_{b2} are stiffness constants of springs linking the upper body masses to the backrest and constrained to translate along y-axis, and c_{b1} and c_{b2} are the corresponding viscous damping coefficients.

3.1. Model parameters identification

The parameters for the proposed model are identified through minimization of a weighted error function of the model and target APMS responses at the seat pan and the backrest using the optimization function *fmincon* available within Matlab. The minimization is performed for the two different postures determined by the hands position, LAP and SW. The target responses are taken as the mean seat pan and backrest APMS

data obtained for the particular posture. The error function is defined as

$$E(\chi) = \min\left[E_p(\chi) + E_b(\chi)\right], \tag{12}$$

where $\chi = \{\mu_0, \mu_1, \mu_2, \omega_1, \omega_2, \xi_1, \xi_2, \omega_{b1}, \omega_{b2}, \xi_{b1}, \xi_{b2}\}$ is the model parameters vector to be identified. $E(\chi)$ is the error function, and $E_p(\chi)$ and $E_b(\chi)$ are the squared errors resulting from APMS response at the seat pan and the seat back, respectively, taken at various discrete frequencies in the 0.5–40 Hz range, such that

$$\begin{aligned} E_p(\chi) &= \psi \sum_{i=1}^{n} \left[\left|\bar{M}_p^*(\omega_i)\right| - \left|\bar{M}_p(\omega_i)\right|\right]^2 + \sum_{i=1}^{n} \left[\left|\phi_p^*(\omega_i)\right| - \left|\phi_p(\omega_i)\right|\right]^2, \\ E_b(\chi) &= \rho \sum_{i=1}^{n} \left[\left|\bar{M}_b^*(\omega_i)\right| - \left|\bar{M}_b(\omega_i)\right|\right]^2 + \sum_{i=1}^{n} \left[\left|\phi_b^*(\omega_i)\right| - \left|\phi_b(\omega_i)\right|\right]^2, \end{aligned} \tag{13}$$

where $\bar{M}_\lambda^*(\omega_i)$ and $\bar{M}_\lambda(\omega_i)$, $\lambda = p, b$ are the magnitudes of normalized APMSs derived from the model and the measured data, respectively, corresponding to discrete frequency ω_i. $\phi_\lambda^*(\omega_i)$ and $\phi_\lambda(\omega_i)$ are the corresponding APMS phase responses, and n is the number of discrete frequencies selected in the 0.5–40 Hz frequency range, and ψ and ρ are the weighting factors used to obtain convergence and to ensure somewhat comparable contributions of the magnitude and phase errors in the error function. The error function $E(\chi)$ was computed from the weighted error functions in Eq. (13), which evaluated at the center frequencies of the third-octave bands in the 0.5–40 Hz frequency range.

The error function in Eq. (12) was minimized subject to a number of inequality constraints imposed on the model parameters. Limit constraints were applied to the model masses to ensure that the total model mass is close to the mean normalized static force measured at the seat pan corresponding to the posture considered, as summarized in Table 2. Assuming that masses m_1 and m_2 represent the upper body mass supported by the backrest, the normal component of the masses acting on the backrest was constrained around the measured values of 30.4% and 28.1% of the body mass for the LAP and SW postures. The limit constraints were defined to allow these masses to vary within a narrow band of $\pm 4\%$, such that

$$\begin{aligned} &0.735 \leqslant \sum_{i=0}^{2} \mu_i \leqslant 0.797 \\ &0.292 \leqslant (\mu_1 + \mu_2)\sin\alpha \leqslant 0.316 \end{aligned} \quad \text{for LAP posture,} \tag{14}$$

$$\begin{aligned} &0.706 \leqslant \sum_{i=0}^{2} \mu_i \leqslant 0.764 \\ &0.270 \leqslant (\mu_1 + \mu_2)\sin\alpha \leqslant 0.292 \end{aligned} \quad \text{for SW posture.} \tag{15}$$

The above minimization problem was solved for different starting values of the parameter vector χ, which resulted in very similar solutions for non-dimensional model parameters.

4. Results and discussions

4.1. APMS responses measured at the seat pan and the backrest

Figs. 5 and 6 illustrate comparisons of APMS responses of 24 seated subjects measured at the pan and backrest, respectively, under broad-band vertical vibration (0.5 m/s^2 rms acceleration) for both sitting postures, LAP and SW. The results show mean responses for each subject derived from data acquired for two repeats under each test condition. The results show considerable scatter in both the pan and the back magnitude data. The scatter in the magnitude response tends to be higher at lower frequencies, which can be partly attributed to variations in the body masses. The dispersion of the measured data tends to be larger for the backrest. Despite the dispersion of the data, the results suggest consistent trends in both the magnitude and the phase responses for both postures in the entire frequency range, particularly with regards to the fundamental resonant frequency. The primary peaks in the seat pan as well as backrest APMS magnitudes occur in the 6.5–8.6 Hz and 5.1–8.2 Hz ranges for the LAP and SW postures, respectively. The backrest APMS

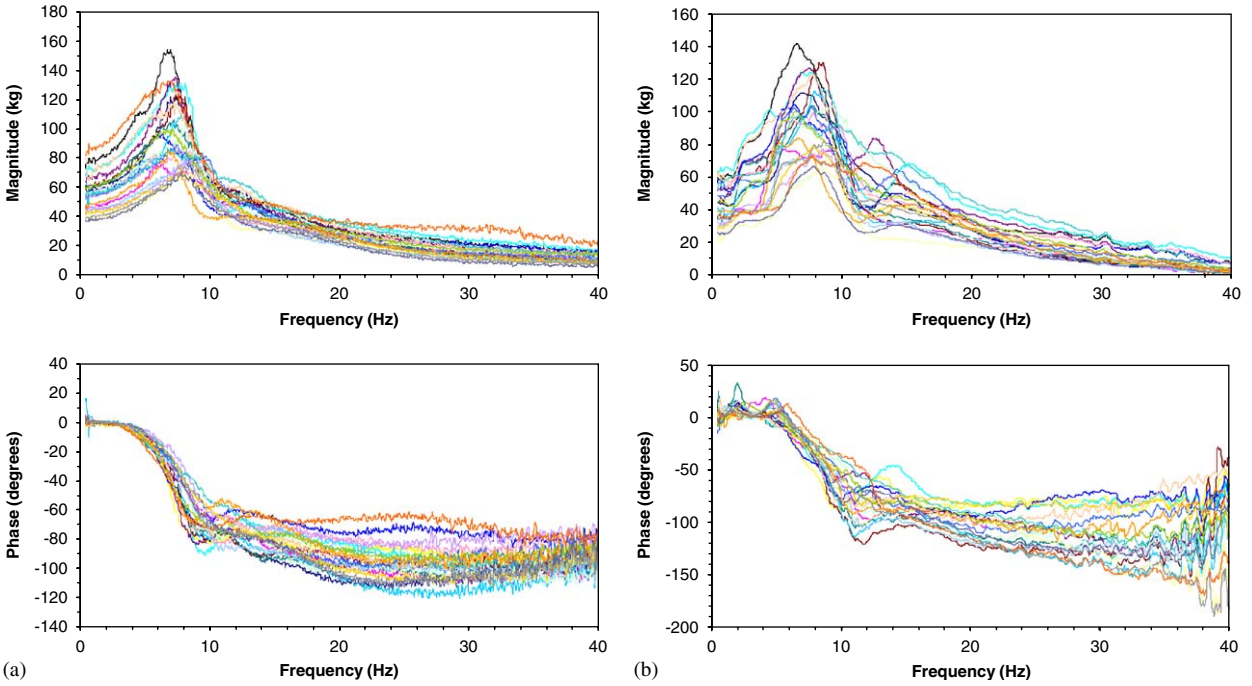

Fig. 5. Comparisons of APMS responses of 24 subjects measured at the seat pan and the backrest (Posture—LAP; excitation—0.5 m/s^2 rms): (a) seat pan; (b) backrest.

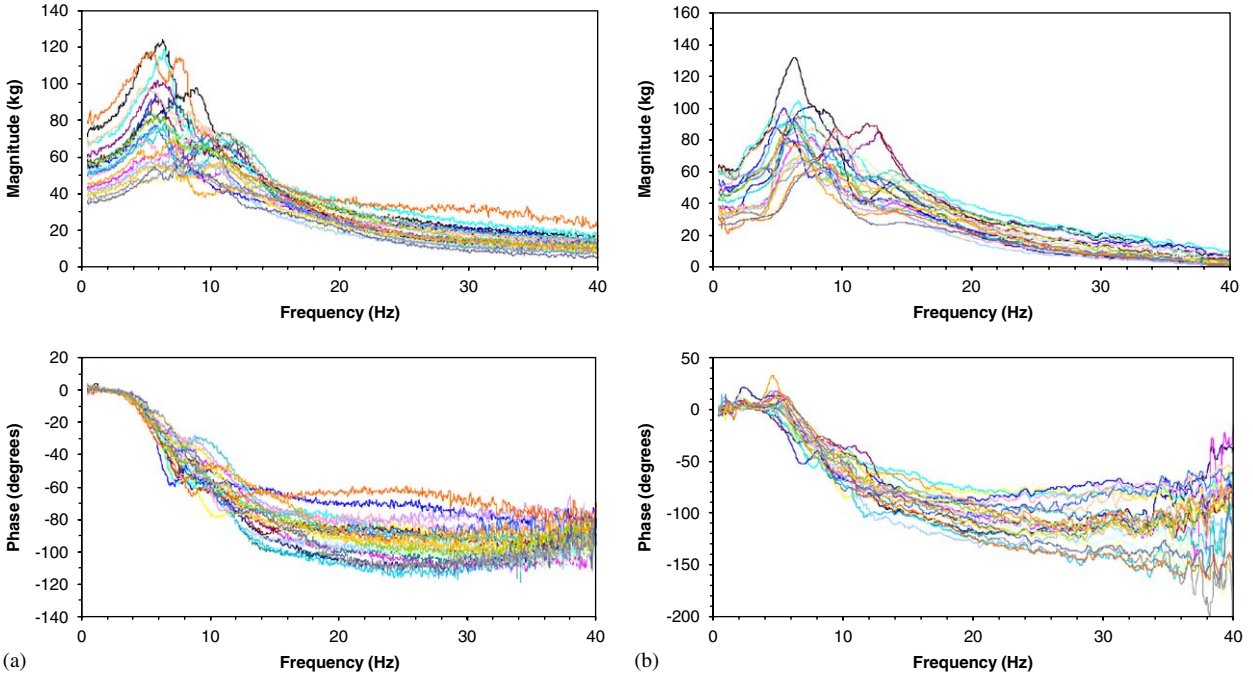

Fig. 6. Comparisons of APMS responses of 24 subjects measured at the seat pan and the backrest (Posture-SW; excitation—0.5 m/s^2 rms): (a) seat pan; (b) backrest.

magnitude responses, however, show the presence of secondary resonance peak more clearly in the 10–15 Hz range. The backrest magnitude and phase responses exhibit considerably larger variability in the higher frequency range than that observed in the seat pan response. This may be attributed to variations in the contact force between the upper body and the backrest. The magnitude of backrest APMS tends to be considerably smaller than that of the pan at lower frequency, which is attributed to the lower portion of the seated body mass supported by the backrest under static conditions. The peak backrest magnitude, however, is comparable to that measured at the seat base. These results suggest considerable dynamic interactions of the upper body with the backrest in the direction normal to the back support, even though the excitation is applied along the vertical axis. This could be attributed to rotational motions of the upper body, which has been widely observed under vertical vibration [11–15].

The measured data are normalized with respect to a measure of the body mass in order to reduce the variations caused by differences in the body mass and to facilitate interpretations with respect to the role of other contributing factors. The measured seat pan APMS magnitude data for each subject are normalized with respect to the mass of the same subject supported by the pan, using the results summarized in Table 2. The backrest APMS magnitude data for each subject is normalized with respect to the upper body mass, assuming that the entire upper body contributes to the dynamic force developed at the backrest. The reported anthropometric data suggests that the human upper body mass, including the masses due to head, neck, trunk and arms, accounts for nearly 67.8% of the total body mass for the LAP posture, and 65.6% for the SW posture [24]. These proportions yield normal components of the static force on the inclined backrest as 27.6% and 26.7%, respectively, which are only slightly lower than the measured values (Table 2). Fig. 7 illustrates both the pan and back APMS normalized magnitude responses of the subjects seated assuming LAP and SW postures and exposed to 0.5 m/s^2 excitation. The results show nearly unity values of both magnitudes at low frequency of 0.5 Hz.The normalized magnitude responses at the seat pan generally exhibit a single peak in the 6.5–8.6 Hz frequency range under LAP posture, and two peaks in the 5.1–8.2 Hz and 10–15 Hz ranges for the SW posture. The normalized backrest magnitude responses reveal a peak near 2 Hz for some of the subjects, which may be associated with the pitch rotation of the upper body [9,18], while the majority of the data sets

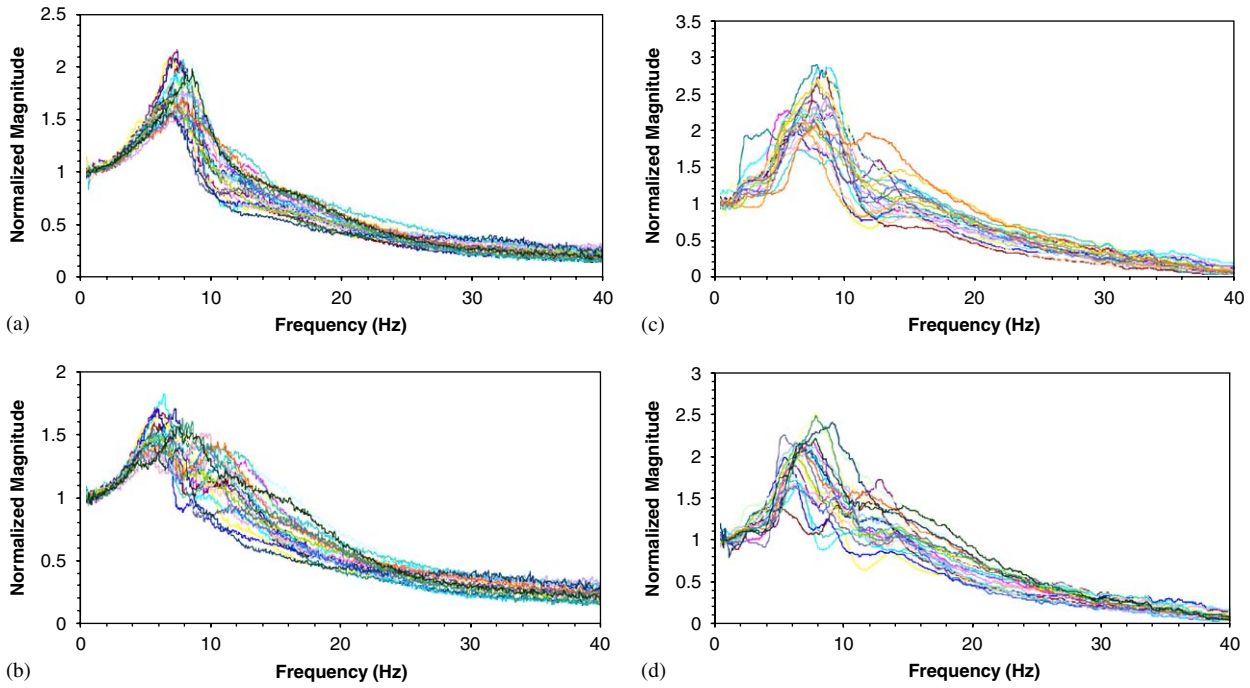

Fig. 7. Comparisons of normalized APMS responses of 24 subjects measured at the seat pan and the backrest under two postures (excitation—0.5 m/s^2 rms): (a) seat pan-LAP; (b) seat pan-SW; (c) back support—LAP; and (d) back support—SW.

show two distinct peaks in the 5.5–9.5 Hz and 10–15 Hz ranges for both postures. The normalized data reveal relatively large variations in the vicinity of the fundamental resonant frequency. The peak standard deviation for the normalized pan magnitude data was observed to be in the order of 16% and 18% for the LAP and SW postures, respectively. The normalized backrest data revealed peak standard deviation of the mean in the orders of 21% and 24% for the LAP and SW postures. The higher variability in the backrest APMS is most likely caused by inconsistent contact of the upper body with the backrest.

4.2. Influence of body mass

The trends observed in magnitude data suggest that the peak values of both the seat pan and backrest responses increase with increasing body mass, as illustrated in Fig. 8 for the two postures, while the corresponding frequency generally tends to decrease slightly. Despite the considerable dispersion in the magnitude data, the peak seat pan and backrest APMS magnitudes could be positively correlated with the body mass ($r^2 > 0.8$), while the correlation with frequency was observed to be considerably lower. Such trends have been widely observed for the vertical APMS magnitude measured at the seat base [13,15]. The results show similar variations in the vertical APMS measured at the seat base and that measured at the back along an axis normal to the backrest with the body mass. Moreover, the peak magnitude of backrest APMS is close to or slightly higher than that of the seat pan.

Owing to the strong influence of the body mass on the APMS responses, the measured data are grouped in four different body mass ranges, which resulted in 8, 5, 6 and 5 data sets within the body mass ranges below 60, 60.5–70, 70.5–80 and above 80 kg, respectively. The respective mean masses for the four groups were obtained as 53.4, 67.6, 75.1 and 97.4 kg. Considering relatively smaller effects of magnitude of vibration excitations, when compared to those caused by variations in the hands position and the body mass, the data acquired under three different magnitudes of broadband vibration are combined to derive the mean responses for the four mass groups, as illustrated in Fig. 9. The mean curves are considered to represent the body weight-dependent biodynamic behaviors of the seated occupants measured at the seat base and the backrest, while

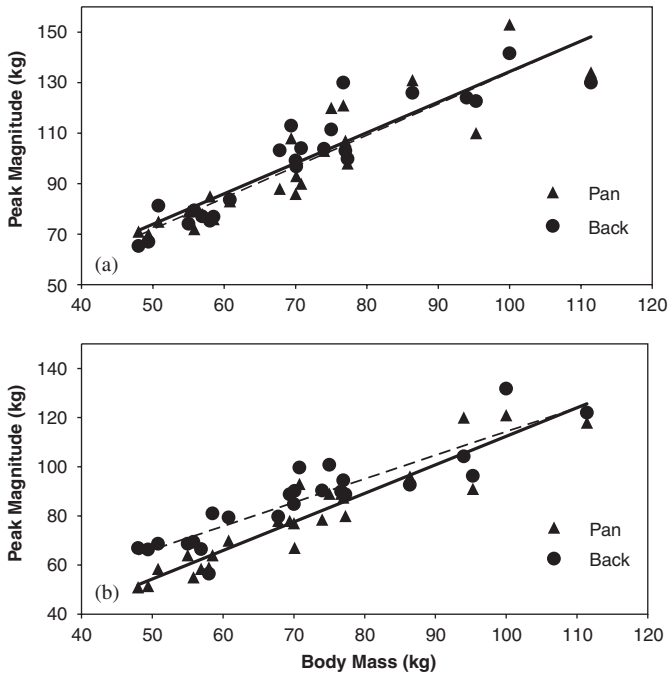

Fig. 8. Variations in peak pan and backrest APMS magnitudes with total body mass: (a) LAP posture; (b) SW posture (—▲—, seat pan; – –●– –, backrest).

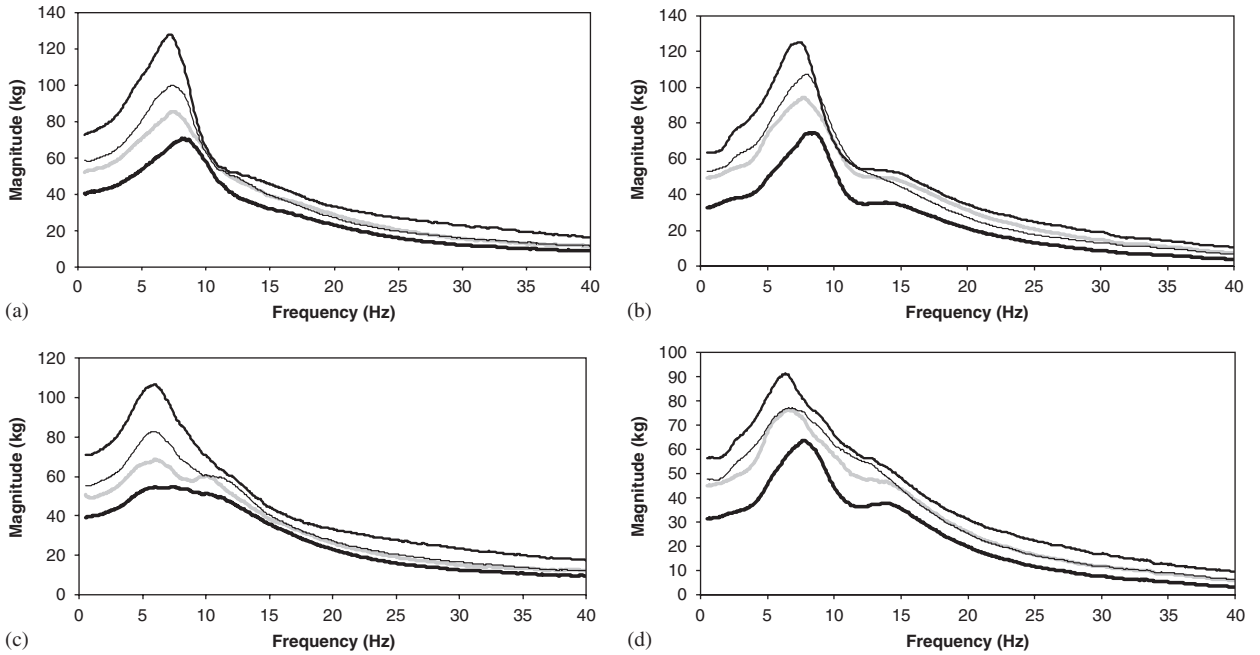

Fig. 9. Mean-APMS magnitude responses measured at the pan and the backrest as a function of the body mass and the hands position: (a) seat pan—LAP; (b) backrest—LAP; (c) seat pan—SW; (d) backrest—SW (▬, below 60; ▬, 60.5–70.5; ▬, 70.5–80; ▬, above 80 kg).

assuming passenger- and driver-like postures in automobiles, and exposed to vertical vibration in the 0.25–1.0 m/s^2 rms acceleration in the 0.5–40 Hz range.

4.3. *Influence of type and magnitude of vertical vibration*

The mean magnitude responses of 24 subjects measured at the seat pan and the backrest, obtained for three different magnitudes of broad-band random excitations, and a track-measured excitation (rms acceleration = 1.07 m/s^2) are compared in Figs. 10 and 11, respectively, for the LAP and SW posture. The results show that the peak APMS magnitudes measured on the seat pan and the backrest, and the corresponding frequency decrease slightly as the magnitude of broad-band excitation increases. The variations in the peak magnitude and the corresponding frequency of the mean APMS response of the occupants seated with SW posture are observed to be considerably smaller than those observed for the LAP posture. Moreover, the magnitude responses attained under track-measured excitations are comparable with those attained under 1 m/s^2 white-noise excitation, while some differences in the phase response are observed at higher frequencies, which could be attributed to significantly lower magnitude of track-induced vibration in the high frequency range. The mean responses suggest relatively small influences of magnitude and type of excitation considered in this study, although the variations in magnitude and the corresponding frequency reveal nonlinear nature of the response, which has been observed in a number of reported studies for the seat pan APMS responses [2,12,13].

As for the mean APMS magnitudes on seat back of 24 subjects for both postures, there is only little influence of magnitude of excitation on the first peak magnitude but the secondary peak magnitude and the corresponding frequency decrease slightly as the magnitude of excitation increases. For hands-on-steering wheel posture, the mean magnitude response curves consistently reveal the presence of a distinct second peak in the 12–15 Hz frequency range. The mean phase response tends to be lower at frequencies above 20 Hz under the track-measured excitation, which is most likely attributed to considerably lower magnitude of vibration at higher frequencies.

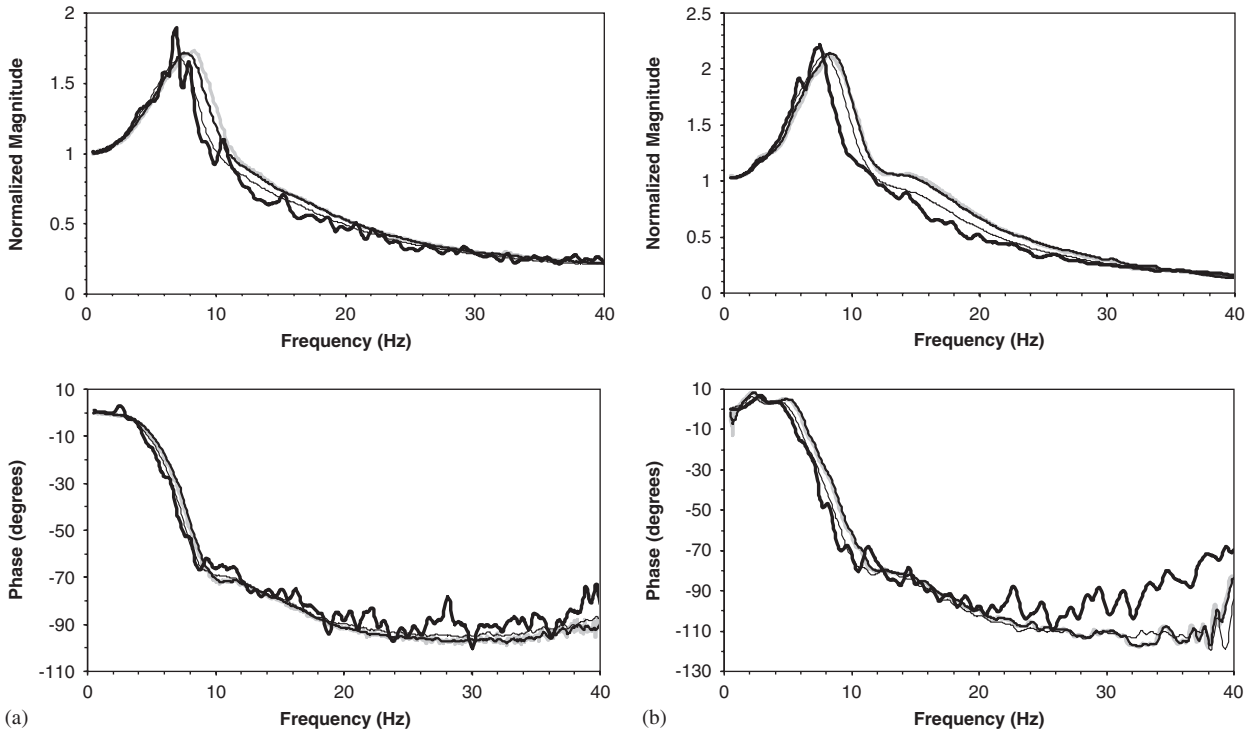

Fig. 10. Comparisons of mean normalized APMS responses measured at the seat pan and the backrest under white-noise and track-measured random excitations (posture—LAP): (a) seat pan; (b) back support (▬, track-measured: ▬, 0.25; ▬, 0.5; ▬, 1.0 m/s^2).

4.4. Influence of hands position

In light of only slight variations in the mean magnitude and phase response due to different excitations, the mean of mean data sets is considered to represent the mean biodynamic response of the 24 subjects under different levels and types of vibration excitations. Owing to the strong influence of hands position, two means of mean data sets are derived corresponding to LAP and SW postures for both pan and the backrest APMS responses, which could serve as the target mean functions for development of mechanical equivalent models. Fig. 12 illustrates comparisons of the APMS responses measured at the seat pan and the backrest for the LAP and SW postures. The results clearly show important differences due to the two hands positions on the mean APMS magnitude responses measured at the seat pan and the backrest, while the effect on the mean phase response is very small. The influence of hands position on the backrest APMS magnitude is similar to that observed for the vertical APMS response, which has been reported in [13]. The mean magnitude at the pan reveals a single-degree-of-freedom-like behavior for the LAP posture with resonant frequency in the vicinity of 7.9 Hz, while that at the backrest shows the primary peak near 8.1 Hz and an additional secondary resonance near 14.5 Hz.This may relate to the interactions associated with the upper body mode. The mean magnitude response for the SW posture exhibits the presence of both modes in the pan as well as backrest responses, occurring around 6.5 Hz for the pan and 7.1 Hz for the back, and 12–14 Hz. The results also show that these frequencies corresponding to the peak magnitudes at the back support are slightly higher than those observed from the mean pan magnitude response.

4.5. Identification of target response functions and model parameters

Owing to the strong influences of hands position on the seat pan as well as backrest APMS magnitudes, the results presented in Fig. 12 could serve as the target functions for identifying the model parameters. Two sets

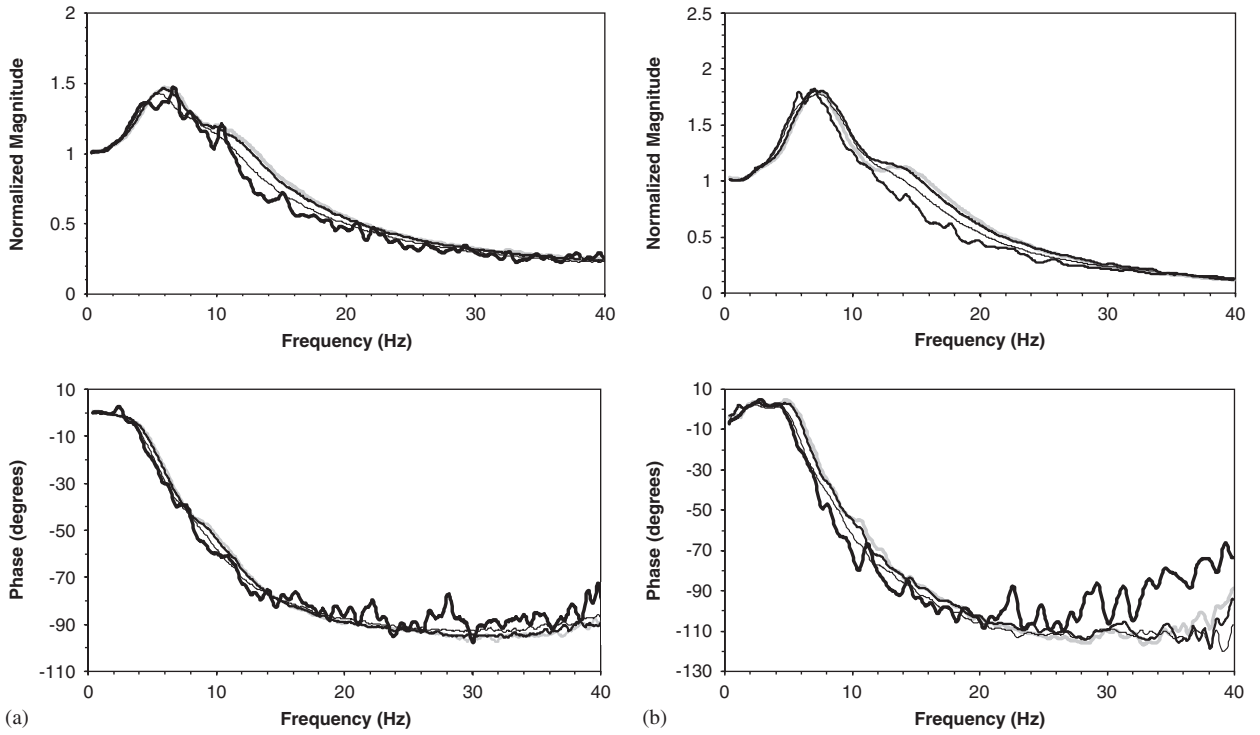

Fig. 11. Comparisons of mean normalized APMS responses measured at the seat pan and the backrest under white-noise and track-measured random excitations (posture—SW): (a) seat pan; (b) back support (▬, track-measured: ▬, 0.25; ▬, 0.5; ▬, 1.0 m/s^2).

of parameters are identified for models applicable for the two hands positions and mean body mass of 71.2 kg, which are summarized in Table 3. Fig. 13 illustrates the comparisons of seat pan and backrest APMS responses derived from the models with the corresponding target values. The masses m_1 and m_2, and the total model mass obtained for SW hands posture are lower than those for LAP model, which conforms with the measured data summarized in Table 2. The stiffness coefficients of the SW model are also lower than those identified for the LAP model, while the corresponding damping coefficient are higher with the exception of c_{b2}, which are attributed to lower fundamental frequency and peak magnitudes of the mean seat pan and backrest APMS corresponding to the SW posture.

Eigenvalue analyses of the identified models revealed two modes for the seat pan responses with resonant frequencies of 7.8 and 15.7 Hz, and corresponding damping ratios of 0.46 and 0.29 for the LAP posture. The corresponding frequencies and damping ratios for the SW posture model were identified as 6.5, 13.7 Hz, 0.52 and 0.46. The first mode for both the models revealed predominant motions of mass m_2, while the second mode suggested that of mass m_1. The resonant frequencies related to the upper body biodynamic responses were obtained as 8.1 and 13.8 Hz with respective damping ratios of 0.22 and 0.34 for the LAP model. The corresponding frequencies for SW model were attained as 7.08 and 13.5 Hz with respective damping ratios of 0.28 and 0.30. These results suggest that the model responses would yield slightly higher first mode frequency of the backrest than for the seat pan, while the second mode frequency of the backrest response is lower.

The APMS magnitude and phase responses of the models at the seat pan and the backrest show reasonably good agreements with the corresponding mean measured data for both the LAP and SW hands postures, as evident in Fig. 13. The seat pan responses of the models are in close agreement with the mean measured responses, while those of the backrest reveal some differences, particularly in the phase responses for both hands positions, which could in-part be attributed to relatively inconsistent contact between the upper-body and the backrest as observed from relatively high inter-subject variations. The identified models are considered to characterize the mean biodynamic response of human occupants with body mass in the vicinity of 71.2 kg, and seated with the back supported against an inclined backrest with hands in lap and on the steering wheel.

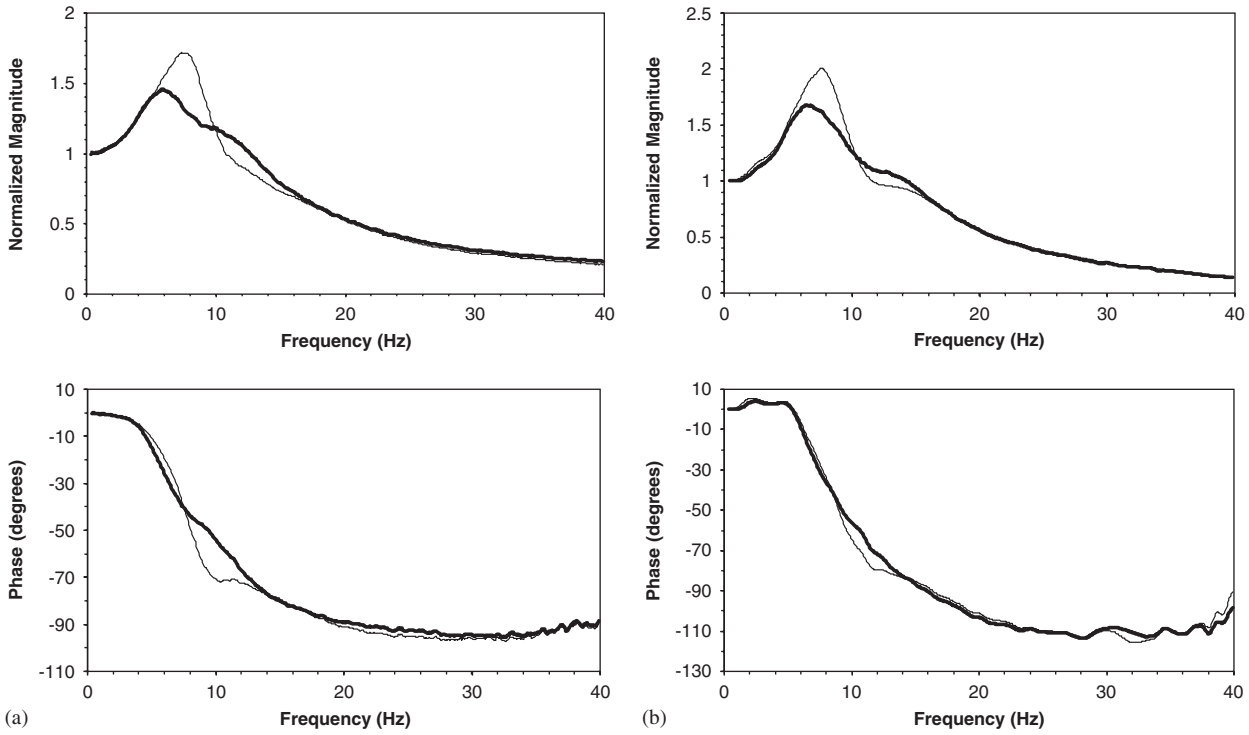

Fig. 12. Influence of hands position on the mean APMS responses of seated occupants: (a) seat pan APMS; (b) backrest APMS (———, LAP; ▬▬, SW).

Table 3
Parameters of mechanical-equivalent models applicable for mean body mass, LAP and SW hands positions

Parameter	Parameter value	
	LAP posture	SW posture
μ_0 (m_0), kg	0.05 (3.56)	0.05 (3.56)
μ_1 (m_1), kg	0.43 (30.62)	0.42 (29.9)
μ_2 (m_2), kg	0.30 (21.36)	0.28 (19.94)
$\Sigma\mu_i(\Sigma m_i)$,kg	0.78 (55.54)	0.75 (53.40)
k_1, kN/m	306.2	299.0
k_2, kN/m	66.4	42.7
k_{b1}, kN/m	84.4	77.1
k_{b2}, kN/m	159.8	1430.5
c_1, N s/m	1673	1764
c_2, N s/m	946	1047
c_{b1}, N s/m	698	859
c_{b2}, N s/m	1244	1006

Owing to the strong dependency of the biodynamic responses measured at the seat pan and the backrest on the occupant mass, it would be desirable to identify the mechanical-equivalent models that could characterize the APMS responses over a range of body masses. For this purpose, the APMS responses derived for four groups of body masses (Fig. 9) are considered as the target functions for parameter identification. The solutions of the minimization problem resulted in 8 sets of model parameters for the models of seated occupants within the four mass groups, while seated with hands in lap and on steering wheel. The resulting

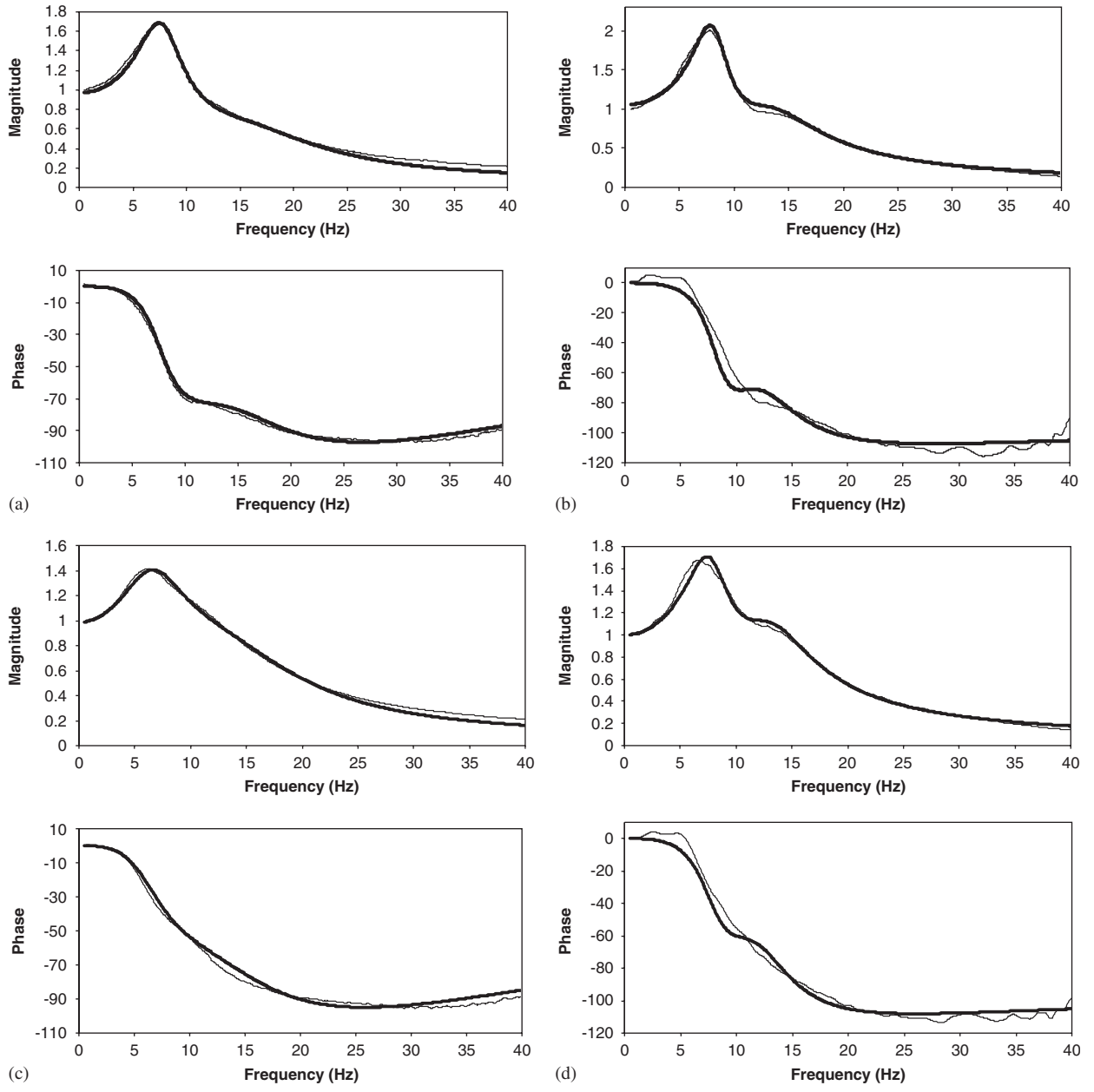

Fig. 13. Comparisons of seat pan and backrest apparent mass responses derived from the LAP and SW models with the corresponding mean measured responses: (a) seat pan—LAP; (b) backrest—LAP; (c) seat pan—SW; (d) backrest—SW (———, mean measured; ———, model).

vectors of non-dimensional parameters are used to derive the model parameters summarized in Table 4. Results suggest that the model masses identified for the four groups increase with increase in the mean body mass and tend to be slightly lower for the SW posture. The stiffness and damping parameters of the models for the groups also increase with the mean body mass, with the exception of k_{b2} for the models corresponding to 60.5–70.5 and 70.5–80 kg mass groups. With the excerption of k_{b2}, the model parameters identified for the mean body mass are close to those for the 70.5–80 kg mass group. This trend in increasing parameter values with the body mass may be used to identify model parameters for specific occupant masses.

Table 4
Model parameters applicable for body mass within the four mass groups and the mean mass, and two hands positions (LAP and **SW)**

Hands position	Parameter	Parameters values				
	Mass range	< 60 kg	60.5–70 kg	70.5–80 kg	>80 kg	Mean
	Mean mass	53.4 kg	67.6 kg	75.1 kg	97.4 kg	71.2 kg
LAP	m_0 (kg)	2.67	3.38	3.755	4.87	3.56
	m_1 (kg)	22.96	29.07	32.29	41.88	30.62
	m_2 (kg)	16.02	20.28	22.53	29.22	21.36
	k_1 (kN/m)	229.6	290.7	300.7	392.2	306.2
	k_2 (kN/m)	54.9	59.2	66.0	83.2	66.4
	c_1 (N s/m)	1198	1360	1700	2551	1673
	c_2 (N s/m)	871	1011	969	1014	946
	k_{b1} (kN/m)	71.6	83.5	88.2	104.3	84.4
	k_{b2} (kN/m)	130.0	165.0	160.8	207.3	159.8
	c_{b1} (N s/m)	427	722	719	944	698
	c_{b2} (N s/m)	759	1236	1240	2468	1244
SW	m_0 (kg)	2.67	3.38	3.755	4.87	3.56
	m_1 (kg)	22.43	28.39	31.54	40.91	29.90
	m_2 (kg)	14.79	18.92	21.03	27.29	19.94
	k_1 (kN/m)	224.3	281.2	295.8	364.3	299.0
	k_2 (kN/m)	34.4	35.4	43.0	58.1	42.7
	c_1 (N s/m)	1173	1762	1763	2683	1764
	c_2 (N s/m)	856	982	1017	1155	1047
	k_{b1} (kN/m)	65.3	69.5	75.3	93.6	77.1
	k_{b2} (kN/m)	117.1	133.5	127.6	157.3	143.5
	c_{b1} (N s/m)	493	822	1022	1535	859
	c_{b2} (N s/m)	580	1005	1017	2018	1006

The validity of the identified models is examined by comparing the model responses with the mean APMS responses of occupants within the corresponding mass group, as illustrated in Figs. 14 and 15, for the LAP and SW postures. The seat pan responses of the models show reasonably good agreements with the mean measured data for all the four mass groups and both hands positions, although some deviations in the responses are evident. Both the model and the mean measured responses exhibit a decrease in the primary resonant frequency and an increase in the modulus with increase in the mean group mass. The seat pan modulus response of the SW model, however, reveals more deviations from the mean measured modulus than that of the LAP model, particularly at frequencies above 10 Hz. The APMS phase response characteristics of the LAP and SW models also exhibit reasonably good agreements with the mean measured data, with some deviations at frequencies above 10 Hz.

Comparisons of model responses in terms of backrest APMS with the mean measured data for the four mass groups show relatively larger deviations in the magnitude responses. Notable differences are observed in the vicinity of primary (6–8 Hz) as well as secondary (10–15 Hz) frequencies. Moreover, the measured data shows the presence of a minor peak near 2 Hz, which has been attribution to the rotational motion of the upper body. The model is unable to predict this peak due to the absence of the rotational mode. The measured phase responses of all the groups deviate considerably from the corresponding model responses at frequencies above 10 Hz, which may be associated with inconsistencies in the upper body-backrest contact under higher frequency vibration.

5. Conclusions

The biodynamic response characteristics of 24 human subjects seated assuming contact with an inclined back support and exposed to vertical vibration, measured at the two driving-points formed by the buttock-pan

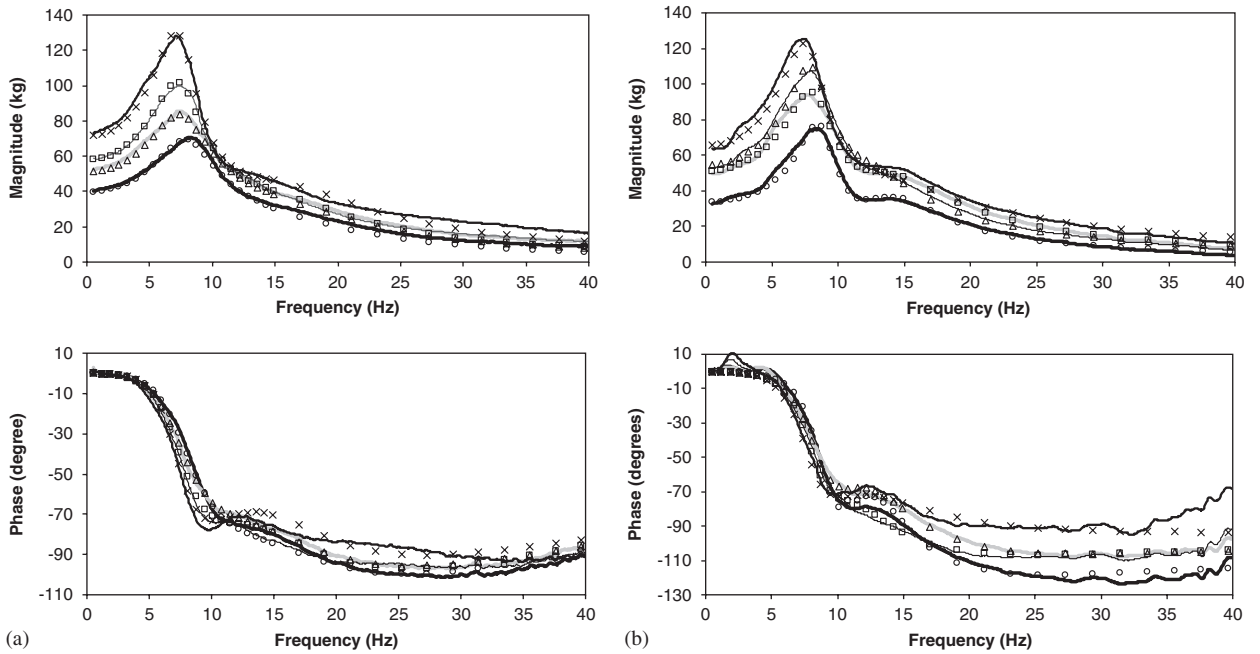

Fig. 14. Comparisons of responses of models for different mass ranges and hands in LAP posture with the corresponding mean measured data: (a) seat pan; and (b) backrest (▬▬, below 60 kg-measured, ○—model; ▬▬, 60.5–70.5 kg-measured, △—model; ▬▬, 70.5–80 kg-measured, □—model; ▬▬, above 80 kg-measured, ×—model).

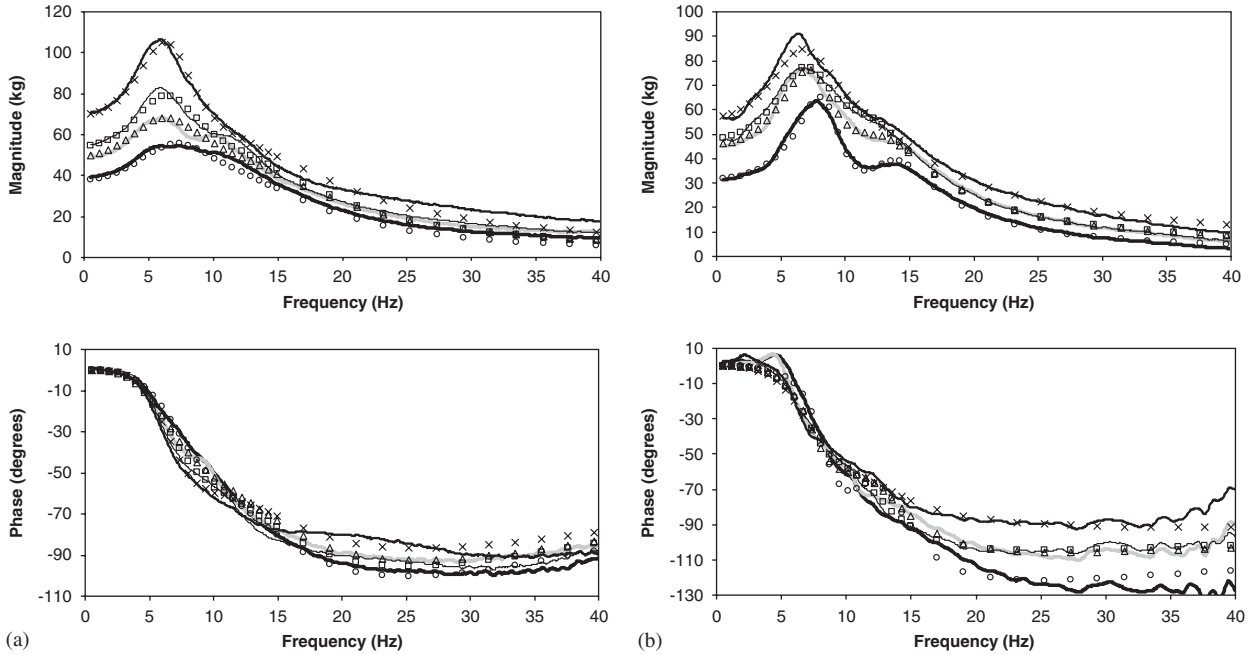

Fig. 15. Comparisons of responses of models for different mass ranges and hands on SW posture with the corresponding mean measured data: (a) seat pan; and (b) backrest (▬▬, below 60 kg-measured, ○—model; ▬▬, 60.5–70.5 kg-measured, △—model; ▬▬, 70.5–80 kg-measured, □—model; ▬▬, above 80 kg-measured, ×—model).

and upper body-back support interfaces, showed important interactions of the upper body with the backrest in a direction normal to the back support surface. Support against an inclined backrest resulted in considerable magnitudes of dynamic forces at the upper body-backrest interface, which is partly attributed to the portion of the body weight supported by the backrest and rotational motions of the upper body caused by vibration at the backrest. The inclined backrest used in this study supported nearly 31.4% of the total body mass, when seated with hands in lap. This proportion reduced slightly to 28.2% when hands were placed on the steering wheel. These proportions corresponded closely to the upper body masses of 67.8% and 65.6% for the hands in lap and on steering wheel postures, respectively, when the backrest geometry was taken into account. The normalization of the backrest APMS magnitudes with respect to these upper body masses helped diminish the wide scatter in the responses at low frequencies, believed to be mostly attributed to variations in the body mass, and resulted in nearly unity magnitudes at low frequencies. This suggested that the entire upper body interacts with the back support along an axis normal to the backrest, even though the vibration was applied along the vertical axis. Considering that the seat pan supported 76.6% and 74.5% of the total body mass for the hands in lap and on steering wheel postures, the upper body masses acting against the backrest would yield most important contributions to the responses measured at the seat pan as well as the backrest. At low frequencies, the APMS magnitudes measured at the backrest were considerably lower than those measured at the seat pan. The backrest APMS magnitudes, however, either exceeded or approached those of the seat pan in the vicinity of the primary resonant frequencies, further suggesting important dynamic interactions with the back support. Such dynamic interactions are mostly caused by the rotational motions of the upper body, which have been widely observed in many studies under vertical vibration.

Despite the considerable scatter in the APMS responses attained for 24 subjects, the normalized magnitude responses at the seat pan revealed a single peak in the 6.5–8.6 Hz range for the hands in lap posture, and two peaks in the 5.1–8.2 and 10–15 Hz ranges for the hands on steering wheel postures. The backrest APMS responses consistently showed the presence of two peaks, irrespective of the hands position, in the 5.5–9.5 and 10–15 Hz ranges. The backrest APMS magnitudes also revealed a minor peak near 2 Hz for most of the subjects, which could be attributed to pitch mode rotation of the upper body. The mean APMS magnitude of the seat pan for the hands in lap posture suggested single-degree-of-freedom-like behavior with primary resonance near 7.9 Hz, which is considerably higher than frequently reported resonant frequency near 5 Hz. The relatively higher resonance frequency observed in this study is ascribed to relatively lower magnitude of vibration and the geometry of the seat, particularly the inclined pan and backrest, and lower seated height. The corresponding mean magnitude of the backrest APMS showed primary peak at a slightly higher frequency, and a secondary peak near 14 Hz. Sitting with hands on the steering wheel generally resulted in relatively lower primary peak magnitude and the corresponding frequency. The mean magnitudes revealed presence of both the modes in the seat pan and backrest responses occurring near 6.5 and 7.1 Hz, and in the 12–14 Hz range. At frequency above 14 Hz, the differences in the APMS magnitudes for the two postures became negligible. The peak magnitudes of the seat pan and backrest APMS magnitudes also increased nearly linearly with the body mass ($r^2 > 0.8$).

The peak APMS magnitudes measured on the seat pan and the backrest, and the corresponding frequency decreased slightly as the magnitude of broad-band excitation increased. The variations in the peak magnitude and the corresponding frequency of the mean APMS response, however, were considerably smaller for the hands on steering wheel posture. This may be due to the stiffening of the body using the additional support provided by the steering wheel. Moreover, the magnitude responses attained under track-measured excitations were comparable with those attained under 1 m/s^2 white-noise excitation, while some differences in the phase responses were evident at higher frequencies, which could be attributed to considerably lower magnitude of track-induced vibration in the high-frequency range. The results thus suggested relatively small influences of magnitude and type of excitations considered in this study, when compared to those caused by variations in the hands position and the body mass.

A four-degrees-of-freedom mechanical-equivalent model was formulated for characterizing the APMS responses of seated occupants exposed to vertical vibration at the two driving-points. Owing to the considerable effects of the body mass and hands position, a total of 8 target functions of the seat pan and backrest APMS were identified involving mean responses of subjects within four different mass groups (<60, 60.5–70, 70.5–80 and >80 kg) and two hands positions. The identified model parameters suggested that the

model masses identified for the four groups increased with increase in the mean body mass and tended to be slightly lower for the SW posture. The stiffness and damping parameters of the models for the groups also increased with the mean body mass, with the exception of k_{b2} for some of the mass groups. This trend could be used to identify model parameters for specific occupant masses.

References

[1] T.E. Fairly, M.J. Griffin, The apparent mass of the seated human body: vertical vibration, *Journal of Biomechanics* 22 (1989) 81–94.

[2] N.J. Mansfield, M.J. Griffin, Effects of posture and vibration magnitude on apparent mass and pelvis rotation during exposure to whole-body vertical vibration, *Journal of Sound and Vibration* 253 (2002) 93–107.

[3] B. Hinz, H. Seidel, The nonlinearity of the human body's dynamic response during sinusoidal whole body vibration, *Industrial Health* 25 (1987) 169–181.

[4] P.M. Donati, C. Bonthoux, Biodynamic response of the human body in the sitting position when subjected to vertical vibration, *Journal of Sound and Vibration* 90 (1989) 423–442.

[5] P. Holmlund, R. Lundstrom, L. Lindberg, Mechanical impedance of the human body in vertical direction, *Applied Ergonomics* 31 (2000) 415–422.

[6] International Organization for Standardization ISO-5982, Mechanical vibration and shock-range of idealized values to characterize seated-body biodynamic response under vertical vibration, 2001.

[7] T. Miwa, Mechanical impedance of the human body in various postures, *Industrial Health* 13 (1975) 1–22.

[8] G.S. Paddan, M.J. Griffin, The transmission of translational seat vibration to the head. Horizontal seat vibration, *Journal of Biomechanics* 21 (1998) 1269–1278.

[9] S. Kitazaki, M.J. Griffin, Resonance behaviour of the seated human body and effects of posture, *Journal of Biomechanics* 31, 143–149.

[10] S.D. Smith, Comparison of the driving-point impedance and transmissibility techniques in describing human response to whole-body vibration, *Proceedings of the UK Group Meeting on Human Responses to Vibration*, Farnborough, UK, 1993.

[11] P.-E. Boileau, S. Rakheja, Whole-body vertical biodynamic response characteristics of the seated vehicle driver: measurement and model development, *International Journal of Industrial Ergonomics* 22 (1998) 449–472.

[12] N. Nawayesh, M.J. Griffin, Effect of seat surface angle on forces at the seat surface during whole-body vertical vibration, *Journal of Sound and Vibration* 284 (2005) 613–634.

[13] W. Wang, S. Rakheja, P.-E. Boileau, Effects of sitting posture on biodynamic response of seated occupants under vertical vibration, *International Journal of Industrial Ergonomics* 34 (2004) 289–306.

[14] G.S. Paddan, M.J. Griffin, A review of the transmission of translational seat vibration to the head, *Journal of Sound and Vibration* 215 (1998) 863–882.

[15] S. Rakheja, I. Stiharu, P.E. Boileau, Seated occupant apparent mass characteristics under automotive postures and vertical vibration, *Journal of Sound and Vibration* 253 (2002) 57–75.

[16] M.J. Griffin, *Handbook of Human Vibration*, Academic Press, London, 1990.

[17] N. Nawayesh, M.J. Griffin, Tri-axial forces at the seat and backrest during whole-body vertical vibration, *Journal of Sound and Vibration* 227 (2004) 309–326.

[18] International Organization for Standardization ISO-WD-108/4 N392, Mechanical vibration—laboratory method for evaluating vehicle seat vibration—specifications of dynamic dummies for z-axis motion, 2002.

[19] M.G.R. Toward, Use of an anthropodynamic dummy to measure seat dynamics, *Proceedings of the 35th UK Group Meeting on Human Responses to Vibration*, 13–15 September, ISVR, University of Southampton, UK, 2000, pp. 39–48.

[20] C.H. Lewis, M.J. Griffin, Evaluating the vibration isolation of soft seat cushions using an active anthropodynamic dummy, *Journal of Sound and Vibration* 253 (2002) 295–311.

[21] N.J. Mansfield, M.J. Griffin, Vehicle seat dynamics measured with an anthropodynamic dummy and human subjects, *Proceedings of the Inter-Noise 96 Congress*, Liverpool, 1996, pp. 1725–1730.

[22] P.E. Boileau, S. Rakheja, X. WU, A body mass dependent mechanical impedance model for applications in vibration seat testing, *Journal of Sound and Vibration* 253 (2002) 243–264.

[23] L. Wei, M.J. Griffin, Mathematical models for the apparent mass of the seated human body exposed to vertical vibration, *Journal of Sound and Vibration* 212 (1998) 855–874.

[24] D.A. Winter, *Biomechanics and Motor Control of Human Movement*, second ed, Wiley, New York, 1990.